Reference force field and charge-density-wave amplitude of mixed-valence halogen-bridged Pt complexes

Alberto Girlando, Anna Painelli, and Marco Ardoino*
Dipartimento di Chimica Generale ed Inorganica, Chimica Analitica e Chimica Fisica, Parma University, viale delle Scienze, 43100 Parma, Italy

Carlo Bellitto
Istituto di Chimica dei Materiali, Consiglio Nazionale delle Ricerche, 00016 Monterotondo Stazione 10, Roma, Italy
(Received 31 October 1994; revised manuscript received 2 February 1995)

The spectroscopic effects of electron-phonon (e-ph) coupling in mixed-valence halogen-bridged chain complexes are investigated through a parallel infrared and Raman study of three compounds with decreasing metal-metal distance along the chain. The e-ph interaction is analyzed in terms of the Herzberg-Teller coupling scheme. We take into account the quadratic term and define a precise reference state. The force field relevant to this state is constructed, whereas the electronic structure is analyzed in terms of a simple phenomenological model, singling out a trimeric unit along the chain. In this way we are able to account for all the available optical data of the three compounds, and to estimate the relevant microscopic parameters, such as the e-ph coupling constants and the charge-density-wave amplitude. The latter correlates linearly with the reciprocal metal-metal distance.

I. INTRODUCTION

Halogen-bridged linear-chain transition-metal complexes (*MX* chains) are characterized by either a charge-density-wave (CDW) or a spin-density-wave (SDW) ground state, the former being the most common.[1-3] In the chemical literature[4] *MX* chains are indeed referred to as mixed valence complexes, a typical formula being $[M^{(IV-\rho)}(L\text{-}L)_2X_2][M^{(II+\rho)}(L\text{-}L)_2]Y_4$, with M=Pt, Pd, Ni; X=a halogen ion; L-L=a bidentate amine ligand; Y=a closed-shell negative counterion, ClO_4^-, Cl^-, etc. The amplitude of the CDW is $\sigma=1-\rho$, and it can be tuned[2,3] by changing the bridging halide, the ligand and/or the counter-ion, thus inducing changes in the crystal packing and/or the hydrogen bond strength. This tunability, together with their crystalline nature, makes *MX* chains useful model systems for testing theories of one-dimensional (1D) solids and in particular to study the interplay between electron-electron and electron-phonon (e-ph) couplings.[5-7] The interest in these compounds is further increased due to the observation of clear spectral signatures of defect states (polarons, solitons, etc.).[7]

On the other hand, whereas the role of e-ph coupling in determining the CDW ground state of *MX* chains has perhaps been overemphasized, its spectroscopic effects have not been fully appreciated. These effects are analogous to those observed in organic charge-transfer (CT) crystals and conjugated polymers,[8] systems to which *MX* chains have often been compared.[5,9] Parallel Raman and infrared (IR) measurements performed on $[Pt(en)_2Cl_2][Pt(en)_2](ClO_4)_4$ (en=ethylendiamine) under pressure[10] have put in evidence some spectroscopic consequences of e-ph coupling. In the present paper we use chemical rather than physical pressure to study spectroscopic effects following a controlled change in CDW strength. In other words, we analyze the ambient pressure Raman and IR data relevant to three members of the so-called PtCl series:

$$[Pt(chxn)_2Cl_2][Pt(chxn)_2](ClO_4)_4\ , \quad (1)$$

$$[Pt(en)_2Cl_2][Pt(en)_2](ClO_4)_4\ , \quad (2)$$

$$[Pt(chxn)_2Cl_2][Pt(chxn)_2]Cl_4 \quad (3)$$

[chxn=(−)(*R*,*R*)−1,2-diaminociclohexane]. As shown in Table I, where the structural data of several PtCl complexes are reported, the ratio r between Pt^{IV}-Cl and Pt^{II}-Cl distances smoothly increases from (1) to (3), in correspondence with a decrease of the Pt^{IV}-Pt^{II} distance. By exploiting the known crystal data,[2,3] we construct a reference force field that, together with a careful analysis of e-ph coupling, allows us to rationalize the main vibrational features of the three compounds and to account for the apparently anomalous behavior of the Pt-Cl stretch-

TABLE I. Interatomic distances along the chain of several PtCl complexes, general formula $[Pt(L\text{-}L)_2][Pt(L\text{-}L)_2Cl_2]Y_4$ (from Refs. 2–4).

	L-L[a]	Y	$d(Pt^{IV}\text{-}Cl)$ Å	$d(Pt^{II}\text{-}Cl)$ Å	$d(Pt^{IV}\text{-}Pt^{II})$ Å	r[b]
(1)	chxn	ClO_4	2.315	3.396	5.711	0.68
	pn	ClO_4	2.29	3.22	5.512	0.71
	$(NH_3)_2$	HSO_4	2.310	3.158	5.466	0.73
(2)	en	ClO_4	2.327	3.101	5.442	0.75
	etn	Cl	2.26	3.13	5.39	0.72
	en	$CuCl_4$	2.328	2.937	5.261	0.79
(3)	chxn	Cl	2.324	2.834	5.158	0.82

[a]Ligand: chxn=(−)(*R*,*R*)-1,2-diaminecyclohexane; pn=1,2-diaminepropane; en=1,2-diamine-ethane (ethylendiamine); etn=ethylamine.
[b]Ratio between the Pt^{IV}-Cl and Pt^{II}-Cl distances.

ing frequencies under chemical or physical pressure. Furthermore, we show that Raman, absorption, and luminescence spectra of the three compounds are rationalized in terms of a phenomenological model of the PtCl electronic structure, properly accounting for *e*-ph coupling. The fit to experimental data yields a reliable estimate of the CDW amplitude. By relating the CDW amplitude of the three compounds with the corresponding structural data, we offer simple empirical criteria to evaluate the CDW amplitude from a limited set of experimental data for complexes within the PtCl series.

II. EXPERIMENT AND RESULTS

The three PtCl compounds were prepared as reported in the literature.[11,12] The IR spectra were obtained by a Bruker IFS66 FT spectrometer, with a Mylar beamsplitter and a dentereted triglycine sulphate (DTGS) detector. For the Raman spectra we used the same spectrometer, coupled with a Bruker photoluminescence module, using a quartz beamsplitter and Si detector. The excitation light was the 647-nm line of a LEXEL K1000 Kr-ion laser. Rejection of the laser line has been achieved by a Kaiser Supernotch filter. The spectral resolution for both IR and Raman is 2 cm^{-1}.

Figure 1 reports the Raman and IR spectra of the powders of the three compounds from 100 to 500 cm^{-1}. In the figure we put in evidence the bands due to the symmetric (Raman) and antisymmetric (IR) Pt-Cl stretching modes, on which most of the following discussion will be based. From the data in the figure it is clear that by increasing the chemical pressure (i.e., by contracting the chain) the Pt-Cl symmetric (ω_s) and antisymmetric (ω_a) stretching frequencies have opposite behaviors: the former decreases and the latter increases. The trend is the same as that observed by increasing the physical pressure.[10] As will become evident below this behavior is a consequence of the *e*-ph coupling.

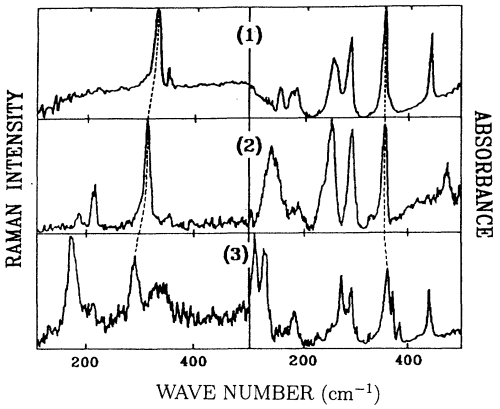

FIG. 1. Raman (left panels) and infrared (right panels) spectra of $[Pt(chxn)_2][Pt(chxn)_2Cl_2](ClO_4)_4$ (1), $[Pt(en)_2][Pt(en)_2Cl_2](ClO_4)_4$ (2), $[Pt(chxn)_2][Pt(chxn)_2Cl_2]Cl_4$ (3) from 100 to 500 cm^{-1}. The dashed lines show the different behaviors of the symmetric (Raman) and antisymmetric (infrared) Pt-Cl stretching with decreasing Pt-Pt distance from (1) to (3).

III. ELECTRON-PHONON COUPLING

1D solids are characterized by the presence of low-lying electronic excitations along the chain direction. The corresponding states strongly interact with the nearby vibrational states, and are responsible for the peculiar vibrational properties of these systems. The spectroscopic signatures of *e*-ph coupling in 1D solids, notably CT organic crystals and conjugated polymers, have been analyzed by a number of authors.[13] We have recently shown[14] that the vibrational spectra of conjugated polymers can be described in terms of the same model adopted for CT organic salts.[15] Here we extend the model to *MX* chains. The essential step in the treatment of such different systems is the proper definition of the reference state, i.e., the state where the perturbation of the vibrational modes due to the low-lying electronic excitations is turned off. The reference state is properly and conveniently defined within a Herzberg-Teller (HT) analysis of *e*-ph coupling, which allows one to account for both linear and quadratic coupling.[14,15] Before specializing the treatment to *MX* chains, we will sketch below the general HT approach to *e*-ph coupling in 1D systems.

In the crude adiabatic approximation the electronic Hamiltonian ($\mathcal{H}_e$) refers to the equilibrium nuclear configuration and does not depend on the nuclear coordinates (Q). The Q dependence is introduced by expanding $\mathcal{H}_e$ on the Q basis. Consistent with the harmonic approximation, the expansion is carried out up to the second order. The *e*-ph Hamiltonian reads

$$\mathcal{H}_{e\text{-ph}}=\Sigma_m \frac{\partial \mathcal{H}_e}{\partial Q_m} Q_m + \tfrac{1}{2}\Sigma_{m,n} \frac{\partial^2 \mathcal{H}_e}{\partial Q_m \partial Q_n} Q_m Q_n \ , \tag{4}$$

where m and n count the phonon coordinates. In the HT scheme $\mathcal{H}_{e\text{-ph}}$ acts as a perturbation on the Q-independent eigenstates of $\mathcal{H}_e$. The ground-state energy corrected up to the second order in Q's (the HT potential) is derived via standard perturbation theory. The second derivatives of the HT potential give the force constants for the nuclear motion:[8,14]

$$\Phi_{mn}=\Phi^s_{mn}+\left\langle G \left| \frac{\partial^2 \mathcal{H}_e}{\partial Q_m \partial Q_n} \right| G \right\rangle - 2\Sigma_F \frac{\langle G|\partial \mathcal{H}_e/\partial Q_m|F\rangle\langle F|\partial \mathcal{H}_e/\partial Q_n|G\rangle}{E_F-E_G} \ , \tag{5}$$

where $|G\rangle$ and $|F\rangle$ are the ground and excited states of $\mathcal{H}_e$, with energies E_G and E_F, respectively, and Φ^s_{mn} represents the skeleton force constants added to account for the contribution of electrons not included in $\mathcal{H}_e$.

The distinctive vibrational properties of 1D systems originate from the last term of Eq. (5); that is, from the linear *e*-ph coupling, which involves the low-lying electronic excitations. This term is strongly dependent on the electronic spectrum, and its contribution cannot readily be rationalized in terms of a traditional vibrational treatment. On the other hand, the contribution from quadratic coupling [the second term in Eq. (5)] only in-

volves the ground state. Then this term is conveniently added to the skeleton contribution to define the reference force field Φ^0_{mn}, which describes the potential due to the core electrons and to the ground-state CT electron distribution, but does not include CT (intervalence) electron fluctuations.[8] It is important to realize that the reference force field, which only accounts for the ground-state electronic distribution, is expected to be transferable among systems with similar ground states, and therefore can be dealt with through the usual vibrational methods.[16]

To apply the above scheme to *MX* chains, the relevant $\mathcal{H}_e$ has to be defined. Although the two-band model proposed by Tinka-Gammel *et al.*[17] has proved useful to show a number of subtle effects, we believe it is unnecessarily complex to account for the phenomena we are dealing with in this paper. So we adopt a one-band model, neglecting the mixing of Pt and Cl orbitals. In the spirit of the crystal-field approximation, we assume that the halogen atoms, bearing a fixed $-|e|$ charge, only act as electrostatic point charges modifying the on-site Pt energies.[6,9] Considering just one *d* orbital per Pt site, the electronic Hamiltonian is written as

$$\mathcal{H}_e = -\varepsilon\Sigma_i(-1)^i n_i + t\Sigma_{i,s}(a^+_{i,s}a_{i+1,s} + \text{H.c.}) + U\Sigma_i a^+_{i,\alpha}a^+_{i,\beta}a_{i,\beta}a_{i,\alpha} + \tfrac{1}{2}\Sigma'_{i,j}V_{ij}q_iq_j \ , \quad (6)$$

where i runs on the metal sites, $s=\alpha,\beta$ is a spin index, $a^+_{i,s}$ ($a_{i,s}$) is the Fermi creation (annihilation) operator for a spin s electron in the ith site, $n_i=\Sigma_s a^+_{i,s}a_{i,s}$ is the number operator for the ith site, and $q_i=4-n_i$ is the corresponding charge operator. Moreover, t is the CT integral between adjacent sites, and U and V_{ij} are the repulsion energies for two electrons residing on the same site or on sites i and j. Finally, ε accounts for the alternation of the on-site Pt energy due to the dimerization of the halogen sublattice.

We now turn our attention to *e*-ph coupling. We neglect the coupling induced by ligand vibrations. This coupling is presumably small, unless the ligand is a charged atom, as in the so-called neutral chains (e.g., $[Pt(en)_2Cl_2][Pt(en)_2Cl_4]$).[4] We are therefore left with the longitudinal modes of the chain. There are three optically active longitudinal modes: Q_s, approximately described as the symmetric Pt^{IV}-Cl stretching, Raman active; Q_a, the corresponding antisymmetric mode, IR active; and

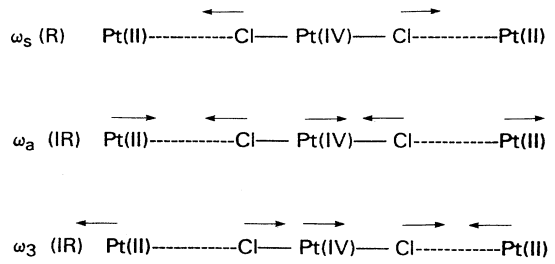

FIG. 2. Approximate description of the zone-center PtCl longitudinal normal modes (from Ref. 4).

Q_3, approximately described as Pt-Pt stretching, IR active. The form of the modes[4] is sketched in Fig. 2. Out of the two IR modes, Q_a is decoupled from the CT electron system, whereas Q_3 modulates on-bond integrals like t (on-bond *e*-ph coupling, *e*-*b*ph). Due to the lack of reliable spectral data in the ω_3 frequency region (see below), we do not discuss the corresponding coupling. On the other hand, due to symmetry reasons,[13] Q_3 does not interact with the Raman Q_s mode. So in the following we will concentrate on the Q_s mode, which is coupled to the electron via a modulation of the on-site energies (on-site *e*-ph coupling, *e*-*s*ph).

We consider the zero-wave-vector Q_s mode. The quadratic *e*-*s*ph coupling is included in the reference frequency, so that the phonon Hamiltonian reads $\mathcal{H}_v=\frac{1}{2}(\omega^0_s)^2Q_s^2$ (here and thereafter we set $\hbar=1$). The linear *e*-*s*ph coupling is dealt with explicitly, the relevant Hamiltonian being

$$\mathcal{H}_{e\text{-}s\text{ph}} = \frac{\partial\mathcal{H}_e}{\partial Q_s}Q_s = \sqrt{N\omega^0_s}\,Q_s g_s\hat{\sigma} \ , \quad (7)$$

where N is the total number of metal sites (twice the number of unit cells) and $\hat{\sigma}=\Sigma_i(-1)^i n_i$ is the site CDW operator. The linear *e*-*s*ph coupling constant g_s is instead defined by $g_s=\sqrt{N/\omega}\,(\partial\varepsilon/\partial Q_s)$.[15] In the spirit of the adopted crystal-field approximation the alternation of the on-site Pt potential (ε) is completely determined by the position of the halogen atoms, so that, assuming an unscreened Coulomb potential between point charges, the *e*-*s*ph coupling constant is given by[9]

$$g_s = \left[\frac{N}{\omega^0_s}\right]^{1/2}\frac{\partial\varepsilon}{\partial Q_s} = \left[\frac{1}{\omega^0_s m}\right]^{1/2}\frac{2e^2}{\pi\varepsilon_0 d^2}\frac{d}{d\xi}\left\{\sum_{i\ \text{odd}}(-1)^{(i+1)/2}\frac{\xi}{i^2-\xi^2}\right\} , \quad (8)$$

where m is the reduced mass of Q_s (equal to the Cl mass), d the Pt-Pt distance, e the electron charge, and ε_0 the dielectric constant. Moreover, the distortion of the Cl sublattice is measured by $\xi=\{d(Pt^{II}Cl)-d(Pt^{IV}\ Cl)\}/d$, related to Q_s through $\xi=2(mN)^{-1/2}Q_s/d$.

In the HT approach the *e*-*s*ph coupling described by Eq. (7) yields a softening of the frequency of Q_s mode according to the equation[13(a),18]

$$\omega_s^2=(\omega^0_s)^2(1-\chi_v g_s^2/\omega^0_s) \ , \quad (9)$$

where χ_v is the electronic response to *e*-*s*ph perturbation:

$$\chi_v = \frac{2}{N}\sum_F\frac{|\langle G|\Sigma_i(-1)^i n_i|F\rangle|^2}{E_F-E_G} \ . \quad (10)$$

We notice that χ_v is a purely electronic quantity, and we are interested in its experimental determination. In

the crystal-field approximation we adopted, the *e*-sph coupling constant g_s is completely determined by the structural data and the reference frequency ω_s^0 [Eq. (8)]. If the latter is known, Eq. (9) allows one to determine the χ_v value from the Raman frequency of the symmetric Pt-Cl stretching mode.

From the discussion following Eq. (5), it turns out that the reference state corresponds to a hypothetical chain with the same CDW amplitude as the actual chain, when the fluctuations of intervalence (CT) electrons (or their effects on the vibrational properties) are turned off. We can therefore construct the reference force field by adopting the standard strategies of vibrational analysis. In particular we start from the force field of the isolated complexes (the core electron contribution) and modify it to account for the actual charge distribution and bond distances inside the chain (the ground-state CT electron contribution). The procedure illustrated in Sec. IV is in many respects analogous to that we have adopted to construct a reference force field for trans-polyacetylene.[14]

IV. REFERENCE FORCE FIELD

Several force fields have been proposed to account for the longitudinal vibrations of *MX* chains.[19–21] The problem looks rather simple, but many alternative choices are possible. A systematic investigation was performed by Bulou *et al.*[21] However, the perturbing effects of *e*-ph coupling [Eq. (9)] were never taken into account. The aim of this section is to determine a reference force field Φ° in the absence of linear *e*-ph coupling. Therefore Φ° is not chosen to fit the ω_s and ω_3 frequencies, which are indeed coupled to the CT electron fluctuations, and the problem is highly undetermined. To overcome this problem we adopt a molecular spectroscopist approach, following Wilson's internal coordinates (GF) scheme.[16]

We start by constructing a force field for the isolated complexes, such as $[Pt(en)_2]Cl_2$ or $[Pt(NH_3)_4Cl_2]Cl_2$, for which extensive vibrational data are available in the literature.[22] We are not interested in vibrations inside the ligand groups, therefore we simplify the structure of the complexes as shown in Fig. 3, in order to get a sensible description of the Pt-N vibrations, the only ones that appreciably couple to Pt-Cl motions. In the figure N* and C* are fictitious atoms, with the mass of NH_2 and CH_3, respectively: In such a way we account for the effect of the H atoms on the N and C motions, without considering the motions of the H themselves. We omit the details of the refinement process that, on the basis of the vibrational data available for the isolated complexes, yielded to the force field reported in Table II. We mention that we made reference to the frequencies of both Pt^{II} and Pt^{IV} complexes, assuming that the ligand's force constants do not depend on the oxidation state of the metal.

Starting from the isolated complexes, four additional internal coordinates are required to describe the $q=0$ vibrations of the linear *MX* chain. Two of them correspond to the motion of Cl atoms out of the line joining the Pt atoms, and a third to the torsion of two neighbor $Pt(N^*C^*)_4$ units. Due to their high masses, vibrations involving these coordinates are probably located below 100

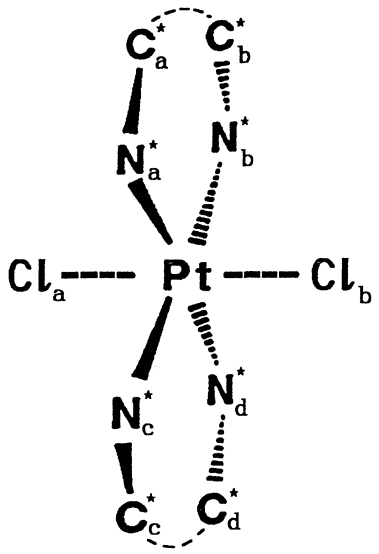

FIG. 3. Schematic representation of the model Pt^{IV} complex used in the normal coordinate analysis. The same structure, without the Cl atoms, is adopted for the Pt^{II} complex.

cm^{-1}, and coupled to the lattice (interchain) modes. Since there are no reliable experimental data to compare with, we arbitrarily attribute to the diagonal force constants corresponding to these three internal coordinates a value of 0.1 mdyn Å/$(rad)^2$, and neglect all off-diagonal interactions. The fourth internal coordinate of the linear chain is the Pt^{II}-Cl stretching coordinate. Of course, we need to fix all force constants involving this coordinate. In particular, by disregarding stretching/bending, bending/bending, as well as stretching/stretching interactions beyond the first-nearest neighbor, we need the following force constants: the diagonal $Pt^{II}Cl$ stretching (K_4), and the two nearest-neighbor interactions: Pt^{IV}-Cl/Pt^{II}-Cl (F_6), and Pt^{II}-Cl/Pt^{II}-Cl (F_7). These three force constants, together with K_3 (Pt^{IV}-Cl stretching) and

TABLE II. Force constants for the isolated model compound.

Symbol[a]	Description of coordinates involved	Value[b]
K_1	Pt-N stretch	2.60
K_2	N-C stretch	5.70
K_3	Pt-Cl stretch	2.00
H_1	N_aPtN_b bend	3.80
H_2	N_aPtN_c bend	0.84
H_3	NPtCl bend	1.05
F_1	Pt-N_a stretch/Pt-N_d stretch	0.63
F_2	Pt-N_a stretch/Pt-N_b stretch	0.35
F_3	Pt-N_a stretch/Pt-N_c stretch	0.10
F_4	Pt-N stretch /N-C stretch	0.50
F_5	Pt-Cl_a stretch/Pt-Cl_b stretch	0.25

[a] K, stretching force constants; H, bending force constants; F, off-diagonal (interaction) force constants.

[b] K and F force constants expressed in mdyn/Å; H, force constants expressed in mdyn Å/$(rad)^2$.

TABLE III. Stretching force constants (mdyn/Å) along the metal-halogen chain for the three studied compounds.

Symbol	Coordinates involved	(1)	(2)	(3)
K_3	Pt^{IV}-Cl stretch	2.00	2.00	2.00
K_4	Pt^{II}-Cl stretch	0.33	0.40	0.55
F_5	Pt^{IV}-Cl stretch/Pt^{IV}-Cl stretch	0.25	0.25	0.25
F_6	Pt^{IV}-Cl stretch/Pt^{II}-Cl stretch	0.12	0.12	0.12
F_7	Pt^{II}-Cl stretch/Pt^{II}-Cl stretch	0.00	0.00	0.00

F_5 (Pt^{IV}-Cl/Pt^{IV}-Cl stretching interaction) determine ω_a, ω_s^0, and ω_3^0, but only the first frequency, being decoupled from CT electron fluctuations, is experimentally accessible. We have then adopted the following approximations. Since the Pt^{IV}-Cl distance does not change appreciably in the three compounds (as well as in the other known PtCl chains), K_3 and F_5 are set to the same value as for the isolated complex. We expect that $F_5 > F_6 > F_7$, and since $F_5 = 0.25$ mdyn/Å, we neglect F_7 (we estimate $F_7 < 0.1$ mdyn/Å). If we assume that F_6 does not change appreciably in the series of the three compounds considered here (we set it to 0.12 mdyn/Å), the value of K_4 (Pt^{II}-Cl stretching) is completely determined by the experimental ω_a value. Tables II and III collect the values of the force constants relevant to the reference force field for complexes (1)–(3). Table IV reports the reference (calculated) and experimental frequencies for the longitudinal vibrations of the PtCl chains.

The reference force field we constructed is also a guide in the assignment of other low-frequency modes of the studied compounds. This task is of little value for the Raman spectra, which show only a few bands. The complete assignment of the IR spectra in the 100–500-cm^{-1} region is reported in Table V. Unfortunately, we are not able to identify the IR band associated with the third longitudinal mode of the PtCl chains, ω_3. The assignment of this mode has already been a matter of discussion: on the basis of polarized data on complex (2), Degiorgi *et al.*[20] associate it either with a 120- or a 137-cm^{-1} band. On the other hand, this interpretation is rejected by Love *et al.*,[23] who propose the assignment to a weak 167-cm^{-1} band. According to our calculations, the reference frequency is around 100 cm^{-1} (Table IV), but the experimental frequency can be well below this value due to the effect of on-bond *e*-ph coupling. Another complication might arise from the coupling to the lattice modes or to the skeletal modes of the ligands. In our opinion a safe assignment of the ω_3 mode requires the analysis of polarized spectra for a series of complexes with different ligands but identical crystallographic structure.

TABLE IV. Reference and experimental longitudinal frequencies (cm^{-1}).

Complex	ω_s^0	ω_s (obs.)	ω_a^0	ω_a (obs.)	ω_3^0
(1)	335	327	352	352	85
(2)	340	312	355	355	92
(3)	350	290	362	362	104

TABLE V. Assignment of the PtCl infrared spectra (500–100 cm^{-1}).

Experimental frequency[a] (1)	(2)	(3)	Calc. freq.[b]	Approx. description[c]
439 *m*	473 *w*	439 *m*	456–457	ν (Pt-N)
		385 *w*		
364 sh	357 sh		356–357	δ (NPtN)
		371 *m*		
352 *s*	355 *s*	362 *m*	See Table V	ν (Pt-Cl) (ω_a)
	352 sh			
287 *m*	292 *s*	293 *m*	269–272	δ (ClPtN)
260 sh	289 sh			
254 *m*	253 *s*	272 *m*	249–252	δ (ClPtN)
	238 sh			
184 *w*				
	188 *w*, br	182 *w*	183–194	δ (ClPtN)
175 *w*				
154 *w*	139 *s*	127 *s*		"external" ligand?
100 *w*		111 *s*		

[a]Frequencies in cm^{-1}. Approximate relative intensities given by *s*, strong; *m*, medium; *w*, weak; sh, shoulder; br, broad.
[b]Frequency interval (cm^{-1}) in the calculations for the three compounds.
[c]The conventional spectroscopic notation is used: ν stands for stretching mode, δ for bending.

Whereas the proposed force field is by no means unique, it provides the required reference for the analysis of the *e*-ph coupling. Furthermore, it offers consistent guidelines for adaptation to different compounds. For instance, the reciprocal Pt^{II}-Cl and Pt^{IV}-Cl stretching force constants all fall on a straight line when plotted against the Pt-Cl distance (Fig. 4). Such behavior is precisely what is expected and found for the stretching force constants of well-established empirical force fields.[24]

V. ESTIMATE OF THE MICROSCOPIC PARAMETERS

Going back to the experimental frequencies of the Pt-Cl stretchings along the chain, we again underline that, whereas the frequency of the antisymmetric vibration (ω_a) increases with chemical pressure [i.e., increases from

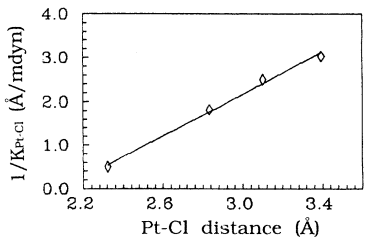

FIG. 4. Plot of the reciprocal Pt-Cl stretching force constants used in the normal coordinate analysis (Table III, K_3 and K_4) vs the Pt-Cl distance.

(1) to (3)] (see Fig. 1 and Table IV), the frequency of the corresponding symmetric stretch (ω_s) does decrease. This counterintuitive behavior can be rationalized *only if* the effects of *e*-ph coupling described by Eq. (9) are accounted for (notice that the reference frequency of the symmetric stretch does increase along the series). In the following we describe a phenomenological model for the electronic structure of Pt-Cl chains which allows us to account for χ_v (i.e., for the vibrational frequencies) as well as for all the other optical data. Thus we can derive reliable microscopic parameters for the three investigated compounds.

We have already remarked[25] that the presence of evident Frank-Condon effects (long progressions in the resonance Raman spectra, marked difference between the absorption and luminescence maxima[2–4]) in the PtCl spectra indicates that the CT exciton is strongly localized. So we attack the problem described by the Eq. (6) Hamiltonian by considering the smallest portion of the chain able to support CT excitons and retaining the complete point symmetry of the infinite chain, namely a trimeric unit $Pt^{II} \cdots ClPt^{IV}Cl \cdots Pt^{II}$. The solution of the Eq. (6) Hamiltonian in terms of the trimer model is reported in the Appendix. Here we observe that the electronic problem of the trimer is fully described in terms of only two parameters. We choose the CT integral (t) and the ground-state site CDW amplitude (σ). Two additional parameters ω_s^0 and g_s are required to describe the phonon part and its coupling to the CT electron. In Sec. IV we showed how ω_s^0 can be estimated by constructing a reference force field through the standard methods of vibrational spectroscopy. Moreover, in Sec. III we showed [Eq. (8)] that in the crystal-field approximation g_s can be evaluated from the structural data in Table I and ω_s^0. Therefore the experimental ω_s frequency (Table IV) yields an umambiguous estimate of χ_v. Within the trimer model χ_v fixes a relation between σ and t [Eq. (A9)]. For each σ and t pair the trimer model allows one to calculate the spectroscopic properties [Eqs. (A10)–(A15)] (Ref. 26) so that the optimal σ and t are derived by fitting the available spectral data for the three studied compounds. In particular we fit the maximum of the absorption intervalence band (ω_{CT}) and of the corresponding luminescence band (ω_L). Moreover, when available, we fit the oscillator strength of the absorption intervalence band (f_{CT}) and the ratio between the intensities of the first overtone over the fundamental band in the resonance Raman spectra. The results of the overall best fit, together with the corresponding microscopic parameters, are reported in Table VI. We observe that the intensity ratio of the resonance Raman bands, which are fitted less satisfactorily than the other quantities, are possibly affected by experimental uncertainties.

TABLE VI. Microscopic parameters and optical data of the three studied compounds (experimental data from present work and Refs. 2–4).

	$[Pt(chxn)_2][Pt(chxn)_2Cl_2](ClO_4)_4$	(1)	
$g_s=0.172$ eV	$\omega_s^0=335$ cm^{-1}	$t=0.27$ eV	$\sigma=0.96$
	ω_s(calc)$=327$ cm^{-1};	ω_s(expt)$=327$ cm^{-1}	
	χ_v(calc)$=0.066$ eV^{-1};	χ_v(expt)$=0.066$ eV^{-1}	
	ω_{CT}(calc)$=3.1$ eV;	ω_{CT}(expt)$=3.2$ eV	
	f_{CT}(calc)$=1.2$;	f_{CT}(expt)$=$---	
	ω_L(calc)$=1.86$ eV;	ω_L(expt)$=1.49$ eV at 2 K	
	$[I(2\omega_s)/I(\omega_s)]$(calc)$=0.56$;	$[I(2\omega_s)/I(\omega_s)]$(expt)$=$---	
	$[Pt(en)_2][Pt(en)_2Cl_2](ClO_4)_4$	(2)	
$g_S=0.188$ eV	$\omega_s^0=340$ cm^{-1}	$t=0.40$ eV	$\sigma=0.87$
	ω_s(calc)$=312$ cm^{-1};	ω_s(expt)$=312$ cm^{-1}	
	χ_v(calc)$=0.188$ eV^{-1};	χ_v(expt)$=0.188$ eV^{-1}	
	ω_{CT}(calc)$=2.68$ eV;	ω_{CT}(expt)$=2.72$ eV	
	f_{CT}(calc)$=2.7$;	f_{CT}(expt)$=3.0$	
	ω_L(calc)$=1.56$ eV;	ω_L(expt)$=1.22$ eV at 2 K	
	$[I(2\omega_s)/I(\omega_s)]$(calc)$=0.45$;	$[I(2\omega_s)/I(\omega_s)]$(expt)$=0.61$, $\lambda_0=2.41$ eV, 80 K	
	$[Pt(chxn)_2][Pt(chxn)_2Cl_2]Cl_4$	(3)	
$g_s=0.206$ eV	$\omega_s^0=350$ cm^{-1}	$t=0.44$ eV	$\sigma=0.78$
	ω_s(calc)$=290$ cm^{-1};	ω_s(expt)$=290$ cm^{-1}	
	χ_v(calc)$=0.321$ eV^{-1};	χ_v(expt)$=0.321$ eV^{-1}	
	ω_{CT}(calc)$=2.20$ eV;	ω_{CT}(expt)$=2.19$ eV	
	f_{CT}(calc)$=3.4$;	f_{CT}(expt)$=$---	
	ω_L(calc)$=1.26$ eV;	ω_L(expt)$=0.91$ eV at 2K	
	$[I(2\omega_s)/I(\omega_s)]$(calc) $=0.45$;	$[I(2\omega_s)/I(\omega_s)]$(expt)$=0.64$, $\lambda_0=2.71$ eV, 80 K	

VI. DISCUSSION AND CONCLUSIONS

It is not at all obvious that a fit with only two free parameters (t and σ) is able satisfactorily to reproduce so many different optical properties [vibrational: ω_s and $I(2\omega_s)/I(\omega_s)$; electronic: ω_{CT} and ω_L, f_{CT}], as reported in Table VI. The overall good fit we obtain for the three compounds shows that the phenomenological trimer model accounts for the fundamental physics of optical excitations in PtCl chains, and thus allows us to get reliable estimates of the corresponding microscopic parameters, and in particular of the CDW amplitude. The latter indeed correlates well with the Pt-Pt distance, that recent local-density-approximation (LDA) calculations[27] indicate as the key parameter controlling the CDW in *MX* chains. Figure 5 shows that a linear correlation exists between the σ values from Table III (stars) and the reciprocal of the Pt-Pt distance. Since the Pt^{IV}-Cl distance is practically constant (Table I), a linear relationship ($\sigma = 1.834 - 1.286r$) also exists between σ and the ratio r between the Pt-Cl distances often quoted in the literature.[4]

The estimate of the CDW amplitude is of paramount importance to determine the properties of *MX* chains. It is therefore interesting to investigate if the diagram in Fig. 5 applies to other members of the PtCl series. In the lack of extensive experimental data we estimate σ for the PtCl complexes listed in Table I from the available structural and vibrational data.[2-4] In particular, the diagram in Fig. 4, that shows the linear relationship between $1/K_{PtCl}$ vs d_{PtCl}, allows us to evaluate K_4 for the PtCl complexes listed in Table I (K_3 is constant) and therefore the reference frequencies ω_s^0. We then evaluate σ by interpolating the differences between the reference frequencies and the experimental frequencies[2-4] (ω_s), and the σ values estimated for compounds (1)–(3) (data in Tables IV and VI). The results are shown as squares in Fig. 5: with the exception of one compound ($[Pt(etn)_4][Pt(etn)_4Cl_2]Cl_4 \cdot 4H_2O$, whose structural data are less accurate[4]), the points fall on the straight line determined above. Analogous results are obtained if the difference between the two experimental frequencies ω_s and ω_a is used to estimate σ. Thus the thorough analysis of the present paper suggests simple but reliable and rather accurate methods to estimate the CDW amplitude from a limited set of experimental data, either structural or vibrational or both.

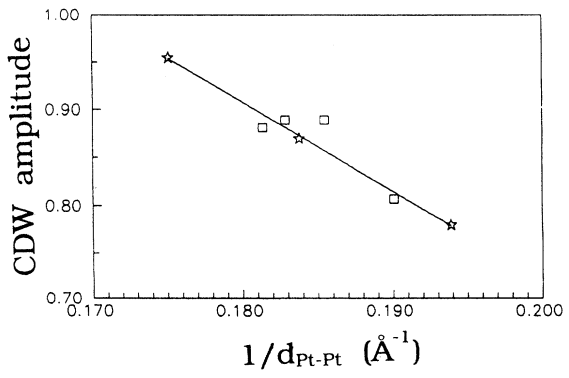

FIG. 5. CDW amplitude estimated for the three studied components (stars) vs the reciprocal Pt-Pt distance. The squares refer to the other PtCl complexes listed in Table I.

The understanding of the role of *e*-ph coupling allows one to explain not only the zone-center spectroscopic data of *MX* solids, but also some features of the phonon-dispersion curves. Through accurate and detailed Raman and IR spectra of isotopically enriched $[Pt(en)_2][Pt(en)_2Cl_2](ClO_4)_4$, Love and co-workers[23,28] unambiguously demonstrated that the complex structure of the Raman-active Pt-Cl stretching mode ω_s (not evidenced in the present study due to the low resolution employed) is due to a Cl isotope effect. Analysis of the data gives information about the width of the phonon-dispersion curves: ω_s should disperse upward by 6.5 cm^{-1}, from zone center to boundary, whereas the dispersion of the corresponding IR-active mode, ω_a, should be less than 3 cm^{-1}.[28] No explanation is offered for this different behavior, and to reproduce it Love and co-workers[23,28] propose a force field with unphysical values for the stretch-stretch interactions ($F_5 - F_7$ in Table III). On the other hand, we know that the ω_s mode is coupled to the electron system, whereas ω_a is not. We believe that the reference (unperturbed) frequency ω_s^0 has a similar dispersion to the ω_a mode. On the other hand, the actual dispersion of the Raman frequency is governed by *e*-ph coupling: $\omega_s(q)$ is given by a generalization of Eq. (9), with the zone center χ_v replaced by the $\chi_v(q)$ function. The q dependence of the susceptibility χ_v cannot be calculated by the trimer model adopted above, but its qualitative behavior is easily understood on simple physical grounds. It is well known that $\chi_v(q)$ of the regular, undistorted chain has a divergence at $q = 2k_F$, as it results from the conventional treatment of the Peierls instability yielding the CDW state.[29] For a half-filled chain $2k_F$ corresponds to the zone boundary, which becomes the zone center after the distortion has taken place. Therefore $\chi_v(q)$ is expected to be maximum at the zone center, as a reminiscence of the Peierls instability, and correspondingly $\omega_s(q)$ is minimum and increases toward the zone edge, as found experimentally.[28]

In the present paper we have shown that the optical properties of *MX* chains, and particularly the opposite behavior of IR and Raman frequencies under physical or chemical pressure, can be understood only if *e*-ph coupling is properly accounted for. We have adopted a simple phenomenological model, but any realistic model for the electronic structure of *MX* chains has to include *e*-sph coupling. In particular, Alouani *et al.*[27] recently fit several properties of Pt*X* chains under uniaxial pressure by neglecting *e*-sph coupling and including a hard-core Pt-*X* repulsion. We believe that, whereas this repulsion is important to account for the nearly constant Pt-*X* distance, a fit including both Raman and IR Pt-*X* stretching frequencies would impose sizable *e*-sph coupling strength.

Summarizing, we have determined several microscopic parameters for PtCl chains by describing the electronic structure in terms of the trimer model. We believe that

this simple model is applicable to all compounds in the PtCl series, given their high-σ values. When intermediate σ values are involved, as in the PtBr and PtI series,[2-4] the trimer model is expected to fail, and should be replaced by more sophisticated models such as the one- or two-band Hubbard models. However, the treatment of the e-ph coupling we have described in the present paper remains applicable, as well as methods followed to describe the phonon part and to construct the reference force field.

ACKNOWLEDGMENTS

Financial support by the Italian Ministry of the University and Scientific and Technological Research (M.U.R.S.T.) and by the National Research Council (C.N.R.) is acknowledged. We thank B. I. Swanson and B. Scott for communicating the results of their work before publication and for useful discussions.

APPENDIX: THE TRIMER MODEL

We consider the smallest portion of chain that retains the point symmetry of the infinite chain, i.e., a trimeric unit $Pt^{II}\cdots ClPt^{IV}Cl\cdots Pt^{II}$ (identical results are obtained with the alternative choice: $Pt^{IV}Cl\cdots Pt^{II}\cdots ClPt^{IV}$). Since PtCl systems are characterized by a large site CDW, we neglect processes like $Pt^{II}\cdots Pt^{IV}\Longrightarrow Pt^{IV}\cdots Pt^{II}$, so that the relevant basis functions are

$$\Phi=|Pt^{II}Pt^{IV}Pt^{II}\rangle ,$$
$$\Psi_{\pm}=\frac{1}{\sqrt{2}}\{|Pt^{III}Pt^{III}Pt^{II}\rangle\pm|Pt^{II}Pt^{III}Pt^{III}\rangle\} , \tag{A1}$$

where within each ket the oxidation state of each Pt indicates the corresponding electronic configuration. The electronic Hamiltonian in Eq. (6) is simplified as

$$\mathcal{H}_e=-2\Delta\hat{\sigma}+t\Sigma_{i,s}(a_{i,s}^{+}a_{i+1,s}+\text{H.c.}) , \tag{A2}$$

where $\hat{\sigma}=1-n_2$. Moreover, 2Δ, the energy difference between $\Psi_{\pm}$ and Φ states, accounts for both the on-site energy alternation (ε) and for electrostatic interactions (U and $V_{i,j}$). $\mathcal{H}_e$ mixes Φ and Ψ_+ states, the corresponding matrix element being $2t$. The solution of the resulting two-state problem (Ψ_- is decoupled) is well known,[30] the corresponding eigenfunctions being

$$\Psi_1=c_1\Phi+c_2\Psi_+$$
$$\Psi_2=c_2\Phi-c_1\psi_+ , \tag{A3}$$
$$\Psi_3=\Psi_- .$$

The site CDW amplitude is measured by $\sigma=c_1^2$, so that it is convenient to describe the electronic problem in terms of the two electronic parameters t and σ. The frequency of the optically allowed CT transition (ω_{CT}^0) and the corresponding transition dipole moments (μ_{CT}^0) are

$$\omega_{CT}^0=2t\left[\frac{\sigma}{1-\sigma}\right]^{1/2} ,$$
$$|\mu_{CT}^0|=ed\sqrt{1-\sigma} . \tag{A4}$$

The e-ph Hamiltonian in Eq. (7) is specialized to the trimeric unit as

$$\mathcal{H}_{e\text{-sph}}=\sqrt{2\omega_s^0}Qg\hat{\sigma} , \tag{A5}$$

where, for the sake of simplicity, we have dropped the s subscript on Q and g. Moreover, we set $N=2$ (we indeed consider just one unit cell). In the adiabatic approximation we substitute Q with its equilibrium value (Q_{eq}) in $\mathcal{H}_{e\text{-sph}}$, and add it to $\mathcal{H}_e$ to get an effective electronic Hamiltonian. The total Hamiltonian is then conveniently written as

$$\mathcal{H}_e+\mathcal{H}_{e\text{-sph}}+\mathcal{H}_{ph}=-2\left[\Delta-\left[\frac{\omega_s^0}{2}\right]^{1/2}gQ_{eq}\right]\hat{\sigma}$$
$$+t\Sigma_{i,s}(a_{i,s}^{+}a_{i+1,s}+\text{H.c.})$$
$$+\sqrt{2\omega_s^0}(Q-Q_{eq})g\hat{\sigma}+\tfrac{1}{2}(\omega_s^0)^2Q^2 . \tag{A6}$$

The first two terms in Eq. (A6) play the role of an adiabatic electronic Hamiltonian with an effective Δ. In other terms, at $Q=Q_{eq}$, the coupled e-ph Hamiltonian has the same solution as the purely electronic Hamiltonian with $\Delta=\Delta_{eff}$. With the help of the Hellmann-Feynman theorem we calculate the first derivative of the ground-state energy of the effective Hamiltonian with respect to Q. By zeroing the derivative we calculate

$$Q_{eq}=-\left[\frac{2}{(\omega_s^0)^3}\right]^{1/2}g\sigma . \tag{A7}$$

The residual e-ph coupling [the third term in Eq. (A6)] is conveniently treated as a perturbation. In other terms, following the HT prescription, we expand the ground-state electronic function around the equilibrium position. We get

$$\Psi_{GS}=\Psi_1-\frac{\sqrt{2\omega_s^0}}{2t}g\sigma(1-\sigma)(Q-Q_{eq})\Psi_2 . \tag{A8}$$

The second derivative of the corresponding HT potential gives the frequency of the ground-state phonon, as reported in Eq. (9) with

$$\chi_v=2[\sigma(1-\sigma)]^{3/2}/t . \tag{A9}$$

On the other hand, Ψ_3 is not perturbed by e-ph coupling, so that the corresponding phonon is not displaced nor softened. So we have two different oscillators in our system: the unperturbed oscillator, relevant to the Ψ_3 state, described by phonon coordinate Q, conjugated momentum P, and frequency ω_s^0; and the ground-state oscillator described by coordinate $q=Q-Q_{eq}$, momentum $p=P$, and frequency ω_s. In the following the n-phonon state relevant to the unperturbed oscillator will be indicated by the ket $|n\rangle$, whereas the n-phonon state relevant to the ground-state oscillator is $|n)$.

We are now in the position to evaluate several optical properties of our model system. Let us start with the CT frequency-dependent conductivity. The corresponding complex conductivity is given by $\sigma_{CT}(\omega)$

$=-ie^2d^2N^d\omega\chi_{CT}(\omega)$, where i is the imaginary unit, N_d is the number of unit cells in the unit volume, and the complex optical susceptibility is

$$\chi_{CT}=\sum_F \frac{2(\omega_F-\omega_G)\langle G|\mu|F\rangle\langle F|\mu|G\rangle}{(\omega_F-\omega_G)^2-\omega^2-i\omega\gamma_F} , \tag{A10}$$

where $|G\rangle=|\Psi_{GS}\rangle|0\rangle$ and $|F\rangle=|\Psi_3\rangle|n\rangle$, ω_F and ω_{CT} are the corresponding energies, and γ_F is the damping factor relevant to $|F\rangle$. By neglecting second-order corrections, the relevant matrix element in Eq. (A10) becomes

$$\begin{aligned}&|(0|\langle\Psi_{GS}|\mu|\Psi_3\rangle|n\rangle|^2\\&\quad=e^2d^2(1-\sigma)(0|n\rangle\langle n|0)\\&\qquad+2e^2d^2\left[\frac{\omega_s^0}{2}\right]^{1/2}\frac{g}{t}[\sigma(1-\sigma)]^{3/2}(0|n\rangle\langle n|q|0) ,\end{aligned} \tag{A11}$$

if q is expressed in terms of the usual phonon creation and annihilation operators relevant to the ground-state oscillator, i.e., $q=(c^++c)/\sqrt{2\omega_s}$. The calculation of the phonon integrals in Eq. (A11) only requires the Frank-Condon factors, $(n|m\rangle$. These factors are easily computed from

$$(0|0\rangle=\sqrt{2}\frac{(\omega_s^0\omega_s)^{1/4}}{(\omega_s^0+\omega_s)^{1/2}}\exp\left\{-\frac{g^2\sigma^2\omega_s}{(\omega_s^0)^2(\omega_s^0+\omega_s)}\right\} , \tag{A12}$$

with the help of the recursive relation (holding for $m>n$):

$$\begin{aligned}2\sqrt{m}\,(n|m\rangle&=(\alpha+1/\alpha)\sqrt{n}\,(n-1|m-1\rangle\\&\quad+(\alpha-1/\alpha)\sqrt{n+1}(n+1|m-1\rangle\\&\quad+2\frac{g\sigma}{\omega_s^0}(n|m-1\rangle ,\end{aligned} \tag{A13}$$

where $\alpha=(\omega_s^0/\omega_s)^{1/2}$. The CT absorption spectrum is proportional to the real part of $\sigma_{CT}(\omega)$. The corresponding oscillator strength is calculated by integration:

$$f_{CT}=\frac{2m_e}{\pi e^2N_d}\int \mathrm{Re}(\sigma_{CT}(\omega))d\omega . \tag{A14}$$

The luminescence spectrum is proportional to the imaginary part of a complex electronic susceptibility, defined by Eq. (A10), but with $|G\rangle=|\Psi_3\rangle|0\rangle$ and $|F\rangle=|\Psi_{GS}\rangle|n\rangle$. Finally, the standard Albrecht theory[30] of the resonance Raman effect allows us to calculate the intensities of the Raman progression bands. In particular the intensity of the $m=0$ vibration is given by

$$I_{m0}\propto(\omega_{ecc}-m\omega_s)^4|\alpha_{m0}|^2 , \tag{A15}$$

where ω_{ecc} is the frequency of the laser radiation, and

$$\begin{aligned}\alpha_{m0}=\sum_F&\left\{\frac{1}{\omega_I-\omega_F-\omega_{ecc}}+\frac{1}{\omega_I-\omega_G-\omega_{ecc}}\right\}\\&\times\langle G|\mu|I\rangle\langle I|\mu|F\rangle ,\end{aligned} \tag{A16}$$

with $|G\rangle=|\Psi_{GS}\rangle|0\rangle$, $|F\rangle=|\Psi_{GS}\rangle|m\rangle$, and $|I\rangle=|\Psi_3\rangle|n\rangle$.

*Present address: Istituto MASPEC-CNR, via Chiavari 18/a, 43100 Parma, Italy.

[1]K. Toriumi, Y. Wada, T. Mitani, S. Bandow, M. Yamashita, and Y. Fuji, J. Am. Chem. Soc. **111**, 2341 (1989); M. Yamashita *et al.*, Synth. Met. **56**, 3461 (1993).

[2]Y. Wada, T. Mitani, M. Yamashita, and T. Koda, J. Phys. Soc. Jpn. **54**, 3143 (1985); H. Okamoto, T. Mitani, K. Toriumi, and M. Yamashita, Mater. Sci. Eng. B **13**, L9 (1992).

[3]B. Scott, R. J. Donohoe, S. P. Love, S. R. Johnson, M. P. Wilkerson, and B. I. Swanson, Synth. Met. **56**, 3426 (1993).

[4]R. J. H. Clark, in *Advances in Infrared and Raman Spectroscopy,* edited by J. H. Clark and R. E. Hester (Wiley, New York, 1984), Chap. 3, p. 95, and references therein.

[5]Y. Onodera, J. Phys. Soc. Jpn. **56**, 250 (1987).

[6]S. Ichinose, Solid State Commun. **50**, 137 (1984).

[7]D. Baeriswyl and A. R. Bishop, J. Phys. C **21**, 339 (1988); S. D. Conradson, M. A. Stroud, M. H. Zietlow, B. I. Swanson, D. Baeriswyl, and A. R. Bishop, Solid State Commun. **65**, 723 (1988); R. J. Donohoe, C. D. Tait, and B. I. Swanson, Chem. Mater. **2**, 315 (1990).

[8]A. Girlando and A. Painelli, Mol. Cryst. Liq. Cryst. **234**, 145 (1993).

[9]A. Painelli and A Girlando, Synth. Met. **29**, F181 (1989).

[10]A. Girlando, A. Painelli, A. Brillante, and C. Bellitto, Synth. Met. **56**, 3407 (1993).

[11]S. Kida, Bull. Chem. Soc. Jpn. **38**, 1804 (1965).

[12]K. P. Larsen and H. Toftlund, Acta Chem. Scand. Ser. A **31**, 182 (1977).

[13]See, for instance, (a) C. Pecile, A. Painelli, and A. Girlando, Mol. Cryst. Liq. Cryst. **171**, 69 (1989); (b) M. J. Rice, Phys. Rev. Lett. **37**, 36 (1976); (c) B. Horovitz, Solid State Commun. **41**, 779 (1982).

[14]A. Girlando, A. Painelli, and Z. G. Soos, Chem. Phys. Lett. **198**, 9 (1992); J. Chem. Phys. **98**, 7692 (1993).

[15]A. Painelli and A. Girlando, J. Chem. Phys. **84**, 5655 (1986).

[16]E. B. Wilson, J. C. Decius, and P. C. Cross, *Molecular Vibrations* (McGraw-Hill, New York, 1955).

[17]J. Tinka Gammel, A. Saxena, I. Batistic, A. R. Bishop, and S. R. Philpot, Phys. Rev. B **45**, 6408 (1992); S. M. Weber-Milbrodt, J. Tinka Gammel, A. R. Bishop, and E. Y. Loh, *ibid.* **45**, 6435 (1992).

[18]A. Painelli and A. Girlando, J. Chem. Phys. **87**, 1705 (1987).

[19]C. E. Paraskevaidis, C. Papatriantafillou, and G. C. Papavassiliou, Chem. Phys. **37**, 389 (1979); C. G. Barraclough, R. J. H. Clark, and M. Kurmoo, J. Struct. Chem. **79**, 239 (1982).

[20]L. Degiorgi, P. Watcher, M. Haruki, and S. Kurita, Phys. Rev. B **40**, 3285 (1989); **42**, 4341 (1990).

[21]A. Bulou, R. J. Donohoe, and B. I. Swanson, J. Phys. Con-

dens. Matter **3**, 1709 (1991).
[22]R. W. Berg and K. Rasmussen, Spectrochim. Acta **28A**, 2319 (1972); D. W. James and M. J. Nolan, J. Raman Spectrosc. **1**, 271 (1973).
[23]S. P. Love, S. C. Huckett, L. A. Worl, T. M. Frankcom, S. A. Ekberg, and B. I. Swanson, Phys. Rev. B **47**, 11 107 (1993).
[24]H. J. Bernstein and S. Sunder, in *Vibrational Spectroscopy, Modern Trends,* edited by A. J. Barnes and W. J. Orville-Thomas (Elsevier, Amsterdam, 1977), p. 413.
[25]A. Girlando and A. Painelli, Synth. Met. **41-43**, 2721 (1991).
[26]We arbitrarily set the damping factor of the excited state, γ_F, to 0.08 eV. The results of the fit are not strongly affected by the chosen value.
[27]M. Alouani, J. W. Wilkins, R. C. Albers, and J. M. Wills, Phys. Rev. Lett. **71**, 1415 (1993).
[28]S. P. Love, L. A. Worl, R. J. Donohoe, S. C. Huckett, and B. I. Swanson, Phys. Rev. B **46**, 813 (1992).
[29]S. Kagoshima, H. Nagasawa, and T. Sambongi, *One-Dimensional Conductors* (Springer-Verlag, Berlin, 1988).
[30]J. Tang and A. C. Albrecht, in *Raman Spectroscopy, Theory and Practice,* edited by A. Szymanski (Plenum, New York, 1970), Vol. 2.